[CANCER RESEARCH 64, 4531–4538, July 1, 2004]

Methylation-Associated Silencing of the *Heat Shock Protein 47* Gene in Human Neuroblastoma

Qiwei Yang,[3] Shuqing Liu,[3] Yufeng Tian,[3] Chiler Hasan,[2] Donna Kersey,[2] Helen R. Salwen,[3] Alexandre Chlenski,[3] Elizabeth J. Perlman,[2] and Susan L. Cohn[1]

Department of [1]Pediatrics and [2]Pathology and [3]The Robert H. Lurie Comprehensive Cancer Center, Northwestern University, Feinberg School of Medicine, Chicago, Illinois

ABSTRACT

Hypermethylation of gene promoter CpG islands is a frequent mechanism for gene inactivation in a variety of human cancers, including neuroblastoma (NB). We demonstrated recently that treatment with the demethylating agent 5′-aza-2′-deoxycytidine (5-Aza-dC) significantly inhibited NB growth *in vivo*. In an effort to identify the genes and biological pathways that are responsible for the impaired NB tumor growth observed after treatment with 5-Aza-dC, we performed genome-wide gene expression analysis of control and treated NBL-W-S NB cells. We found ≥3-fold changes in expression of 44 genes that play roles in angiogenesis, apoptosis, cell adhesion, transcriptional regulation, and signal transduction. The gene encoding heat shock protein 47 (Hsp47), a collagen-specific molecular chaperon, was up-regulated >80-fold after 5-Aza-dC treatment. Expression studies confirmed that *Hsp47* is silenced in a subset of NB cell lines and tumors. We also show that silencing of *Hsp47* in NB cells is associated with aberrant methylation of promoter CpG islands and that *Hsp47* expression can be restored after treatment with 5-Aza-dC. A strong correlation between Hsp47 and collagen type I and IV expression was seen in NB cells. Interestingly, tumorigenicity was inversely correlated with the level of collagen expression in NB cell lines, and higher levels of collagen were detected in mature NB tumors that are associated with favorable outcome compared with undifferentiated, advanced-stage NBs. Our studies support a role for Hsp47 in the regulation of collagen type I and IV production in NB cells and suggest that the level of collagen expression may influence NB tumor phenotype.

INTRODUCTION

The pediatric cancer neuroblastoma (NB) is characterized by a broad spectrum of clinical behavior (1). Although the biological basis for the clinical diversity remains unclear, numerous genetic abnormalities have been shown to correlate with prognosis (2–7). In addition to genetic changes, epigenetic aberrations have also been shown to play an important role in the pathogenesis of most cancers. In NB, hypermethylation of numerous genes has been reported including the angiogenesis inhibitor gene *TSP-1* (8), the CD44 adhesion receptor gene (9), *CASP8* (10), and other genes involved in the tumor necrosis factor-related apoptosis-inducing ligand pathway to apoptosis (11), and the tumor suppressor gene *RASSFIA* (12). Interestingly, a correlation between silencing of *CASP8* and amplification of *MYCN* has been observed (10). In addition, a strong association between *RASSF1A* and *CASP8* methylation in NB has been reported (12), suggesting that multiple genetic and epigenetic abnormalities are likely to influence NB tumor phenotype.

Epigenetic changes can commonly be reversed *in vitro* after treatment with agents that modulate DNA methylation (8–10). In our studies, restoration of *TSP-1* expression was detected in the *MYCN*-amplified NB cell line NBL-W-S within 24 h of 5′-Aza-2′-deoxycytidine (5-Aza-dC) treatment (8). Similarly, other NB cell lines with methylated *TSP-1* responded to treatment, but longer exposure to 5-Aza-dC was required to induce expression. We also found that 5-Aza-dC treatment led to significant inhibition of NB growth *in vivo* and that in a subset of the NB xenografts, *TSP-1* was up-regulated and angiogenesis was impaired (8). However, because 5-Aza-dC is known to globally modulate gene expression, we hypothesized that treatment with this agent affected many other genes that play a role in the regulation of NB tumor growth.

In an effort to identify the genes and biological pathways that are affected by 5-Aza-dC treatment in NB cells, we performed genome-wide gene expression analysis of control and 5-Aza-dC-treated NBL-W-S NB cells. Forty-four genes displayed differential levels of expression (≥3-fold) in the arrays performed with treated *versus* control NB cells. One gene, *SERPINH1* (hereafter referred to as *Hsp47*), the gene encoding Hsp47, was up-regulated >80-fold after 5-Aza-dC treatment. Hsp47, a collagen-specific molecular chaperone, is believed to play an important role in the synthesis, processing, and secretion of collagen (13–17). Our studies demonstrate that *Hsp47* is epigenetically silenced in a subset of NB tumors and cell lines. We also found a strong correlation between *Hsp47* and collagen type I and type IV expression. Interestingly, nontumorigenic NB cell subclones expressed high levels of Hsp47 and collagen, whereas all of the cell lines with low to undetectable levels of Hsp47 protein and collagen are highly tumorigenic in nude mice. High levels of collagen type I expression were also detected in primary tumors with morphological evidence of differentiation, whereas undifferentiated tumors lacked collagen expression, suggesting that collagen may influence NB phenotype.

MATERIALS AND METHODS

Cell Culture and Conditioned Media (CM) Collection. The NBL-W-S cells were cloned from the *MYCN*-amplified NBL-W parental line. The biological characteristics of NBL-W-S and the other NB cell lines used in this study have been described previously (8, 18). NB cell lines and human fibroblasts were grown at 5% CO_2 in RPMI 1640 (Invitrogen, Carlsbad, CA) supplemented with 10% heat-inactivated fetal bovine serum, L-glutamine, and antibiotics. Schwann cells were grown as described previously (19). In some experiments, 5-Aza-dC was added to cells at a final concentration of 1 μM. Cells were harvested at times ranging from 1 day to 5 days of treatment. CM from NB cell lines, human fibroblasts, and Schwann cells were collected and concentrated 20–50-fold using Centricon-3 concentrators (Millipore, Bedford, MA) as described previously (19).

Microarray Analysis. Total RNA was isolated from the 5-Aza-dC-treated and untreated NBL-W-S cell line using TRIzol reagent (Invitrogen) and was cleaned using RNeasy mini columns (Qiagen, Valencia, CA) according to the manufacturer's protocol. cDNA synthesis was performed using the SuperScript Double Stranded cDNA Synthesis kit (Invitrogen). The manufacturer's protocol was modified by the use of an HPLC- purified T7-$(dT)_{24}$ primer (GenSet Oligos; Proligo, Boulder, CO). The double-stranded cDNA product was purified by phenol-chloroform extraction using Phase Lock Gels (Eppendorf Scientific, Westbury, NY) followed by ethanol precipitation. cRNA was syn-

Received 3/19/04; accepted 4/21/04.

Grant support: Neuroblastoma Children's Cancer Society, Friends for Steven Pediatric Cancer Research Fund, the Elise Anderson Neuroblastoma Research Fund, the North Suburban Medical Research Junior Board, and the Robert H. Lurie Comprehensive Cancer Center, NIH, National Cancer Institute Core Grant 5P30CA60553.

The costs of publication of this article were defrayed in part by the payment of page charges. This article must therefore be hereby marked *advertisement* in accordance with 18 U.S.C. Section 1734 solely to indicate this fact.

Requests for reprints: Susan L. Cohn, Children's Memorial Hospital, Division of Hematology/Oncology, 2300 Children's Plaza, Chicago, IL 60614. Phone: (773) 880-4562; Fax: (773) 880-3053; E-mail: scohn@northwestern.edu.

thesized using a BioArray High Yield RNA Transcript Labeling kit (Enzo, Farmingdale, NY) according to the manufacturer's protocol.

In vitro transcription was carried out at 37°C for 5 h, and the biotin-labeled cRNA obtained was purified using the RNeasy Mini kit (Qiagen) and was then fragmented for 35 min at 94°C in 40 mM Tris-acetate (pH 8.1), 100 mM potassium acetate, and 30 mM magnesium acetate. The labeled, fragmented cRNA was added to a 300 μl volume of hybridization mixture, which included final concentrations of 0.1 mg/ml herring sperm DNA (Promega, Madison, WI), 0.5 mg/ml acetylated BSA (Promega), and 2× 4-morpholinepropanesulfonic acid Hybridization Buffer (Sigma, St. Louis, MO). This mixture also included the following hybridization controls: 50 pM of oligonucleotide B2 and 1.5, 5, 25, and 100 pM of cRNA BioB, BioC, BioD, and Cre, respectively (Affymetrix, Santa Clara, CA). We hybridized 250 μl of the mixture to an Affymetrix HG-U133A microarray containing ~22,000 probe sets for 16 h at 45°C in a hybridization oven with constant rotation. The microarrays were washed with nonstringent (6× SSPE, 0.01% Tween 20, and 0.005% Antifoam) and stringent (100 mM 4-morpholinepropanesulfonic acid, 0.1 M NaCl, and 0.01% Tween 20) buffers. The arrays were stained with streptavidin-phycoerythrin (Molecular Probes, Eugene, OR) and the signal amplified using antibody solution. The streptavidin-phycoerythrin stain contained 2× Stain Buffer (final concentration: 100 mM 4-morpholinepropanesulfonic acid, 1 M NaCl, 0.05% Tween 20, 0.005% Antifoam, 2 μg/μl acetylated BSA, and 10 μg/ml streptavidin-phycoerythrin; Molecular Probes). The antibody amplification solution contained 2× Stain Buffer, 2 mg/ml acetylated BSA, 0.1 mg/ml normal goat IgG (Sigma), and 3 μg/ml biotinylated antistreptavidin antibody (Vector Labs, Burlingame, CA).

The arrays were scanned using a fluorometric scanner (HP GeneArray Scanner; Hewlett Packard, Palo Alto, CA) at the excitation wavelength of 488 nm. The scanned images were analyzed using quality control measures established by Affymetrix. Probe signal intensity values were extracted from the array images using Affymetrix Microarray Suite 5.0 software. Data where the presence/absence call was "absent" across all of the samples were excluded. Affymetrix Data Mining Tool 3.0 software was used to calculate fold changes using average signal intensities between groups. Fold change between two comparison groups of ≥3 was used as the cutoff point for comparison.

Expression of *Hsp47* in NB Cell Lines. *Hsp47* mRNA expression in NB cell lines was measured using semiquantitative reverse transcription-PCR. Total RNA (2.0 μg) was reverse-transcribed in a final volume of 20 μl, and 1 μl of the diluted reaction mixture was subsequently amplified by PCR. *Hsp47* sense and antisense primer sequences are shown in Table 1, and β_2-microglobulin was used as a loading control with template diluted 1:500. Each cycle consisted of denaturation at 94°C for 30 s, annealing at 55°C for 30 s, and extension at 72°C for 45 s. The PCR products were subjected to 1.0% agarose gel electrophoresis. The level of Hsp47 and Hsp70 protein was examined by Western blot analysis with mouse monoclonal anti-Hsp47 and anti-Hsp70 antibodies (1:1000 dilution; Stressgen Biotechnologies Inc., San Diego, CA) using methods described previously (8).

Analysis of *Hsp47* Gene Hypermethylation by Methylation-Specific PCR (MSP) and Bisulfite DNA Sequencing. Genomic DNAs were isolated from NB cell lines and tumors using Genomic Tips (Qiagen) and modified by sodium bisulfite using the CpGenome DNA Modification kit (Intergen Co., Purchase, NY). Briefly, 1 μg of genomic DNA was denatured by NaOH and modified by sodium bisulfite, which converts all of the unmethylated cytosines to uracils, whereas methylated cytosines remain unchanged. The modified DNA was desulfonated with NaOH and purified. Primers and PCR conditions used for MSP are shown in Table 1. Q-solution (Qiagen) was added to the reaction mix. Each cycle consisted of denaturation at 94°C for 30 s, annealing at 58°C for 45 s, and extension at 72°C for 45 s. The PCR products were separated by electrophoresis on a 2.5% agarose gel and visualized under UV illumination using ethidium bromide staining. Universal Methylated DNA (Intergen), which is enzymatically methylated human genomic DNA, was used as a positive control for MSP. For bisulfite DNA sequencing, 190-bp PCR products were gel purified and cloned into the pCR2.1-TOPO vector (Invitrogen) according to the manufacturer's protocol. Plasmid DNA was purified with the QIAprep Spin Miniprep kit (Qiagen). Individual plasmids were then sequenced using the ABI PRISM 377 DNA sequencer (Applied Biosystems, Foster City, CA).

Immunofluorescence. NB cells were cultured on coverslips overnight and were then fixed in 1% paraformaldehyde in PBS for 15 min at room temperature. After permeabilization with 70% ethanol for 2 h at -20°C, the coverslips were rinsed and then blocked with 5% nonimmune horse and 5% nonimmune rabbit serum in PBS for 1 h at room temperature. The cells were then incubated with either a mixture of the primary antibodies (5 μg/ml mouse anti-Hsp47 monoclonal IgG; Stressgen) and 1:25 diluted goat anti-type I or IV collagen (Chemicon International, Inc., Temecula, CA). All of the antibody incubations were carried out in PBS containing 5% nonimmune horse serum and 5% nonimmune rabbit serum. Horse antimouse IgG coupled to FITC (Vector Laboratories Inc.) and rhodamine-conjugated rabbit antigoat IgG (Vector) were used as the secondary antibodies at a dilution of 1:200. The coverslips were mounted in a drop of slow anti-Fade (Molecular Probes) to reduce photobleaching. Hoechst dye (Sigma) was used to counterstain nuclei.

Histological sections from a human ganglioneuroma (GNR) were also immunostained using mouse anti-type I collagen (the monoclonal antibody developed by Dr. Heinz Furthmayr was obtained from the Development Studies Hybridoma Bank developed under the auspices of the National Institute of Child Health and Human Development and maintained by the University of Iowa, Department of Biological Sciences, Iowa City, IA) and S-100 (NeoMarkers, Fremont, CA) monoclonal antibodies. Briefly, tumor tissue was fixed in 10% buffered formalin and embedded in paraffin. Four-μm thick sections were rehydrated in graded alcohols and rinsed in PBS. Antigen retrieval was performed with 0.01 M citrate buffer (pH 6.0) in a boiling steamer for 20 min. Sections were incubated with primary anti-pro-α1(I) NH_2-terminal propeptide antibody (1:40) and S-100 (1:100) in a humidity chamber overnight at 4°C, visualized with antimouse fluorescence and Texas Red-labeled horse IgGs (Vector Labs) at room temperature for 30 min. Sections were counterstained and sealed with Vectashield mounting medium with 4′,6-diamidino-2-phenylindole (Vector Labs).

Western Blot Analysis of Type I and IV Collagen. Lysates were prepared from primary tumors as described previously (20), and protein was quantified using the Bio-Rad method (Richmond, CA) following the manufacturer's instructions. Western blot analyses were performed with 10 μg of protein/lane and anti-collagen type I antibody (from the Development Studies Hybridoma Bank; 1:1000 dilution) and anti-collagen type IV antibody [anti-α2 (IV) antibody; 1:500 dilution (Chemicon)] using methods described previously (8). Western blot studies were similarly performed with 10 μg CM, collected from NB cell lines and Schwann cells and concentrated 20-fold using Centricon-3 concentrators (Millipore) as described (8).

NB Xenograft Studies. Female 4–6-week-old homozygous athymic nude mice (Harlan, Madison, WI) were inoculated s.c. into the right flank with 1×10^7 cells from the NBL-W-S cell line. Once tumors were palpable, mice were treated with three doses of 5-Aza-dC (5 mg/kg/dose) in 1 day with 3-h intervals. Mice were sacrificed at day 9 after 5-Aza-dC treatment to analyze Hsp47 re-expression and collagen IV expression at that time point posttreatment. Animals were treated according to NIH guidelines for animal care and use, and protocols were approved by the Animal Care and Use Committee at Northwestern University.

Immunohistochemical Studies. Tumor tissue was fixed in 10% buffered formalin and embedded in paraffin. Four-μm thick sections were rehydrated in graded alcohols and rinsed in PBS. Antigen retrieval was performed with 0.01 M citrate buffer (pH 6.0) in a boiling steamer for 20 min. Sections were incubated

Table 1 *Summary of primer sequences and PCR conditions for detection of Hsp47 methylation status and expression*

Purpose	Forward primer	Reverse primer	AT[a]	Size
MSP1	M: GCGTTTGAAAGGACGTGCGATTCGG	M: CTCGACGACCCGAACTACGAAACG	58	134
	U: GTGTTTGAAAGGATGTGTGATTTGG	U: CTCAACAACCCAAACTACAAAACAC	58	135
MSP2	M: GGAGCGGGTTAAGAGTAGAATCGTGT	M: CCACACACACGCAAACGTCTCCCG	58	109
	U: GGGAGTGGGTTAAGAGTAGAATTGTGT	U: CCACACACACACAAACATCTCCCAC	58	110
Bisulfite sequencing	AGTGGGTTAGTTTATGTAGAGAGTTTGG	CCAAAAACCTCCCTCAAAACCTCCC	55	190
RT-PCR	CTGCAGTCCATCAACGAGTGGGC	GAGATGGCAACAGCCTTCTTCTGC	55	406

[a]AT, annealing temperature; RT-PCR, reverse transcription-PCR.

Table 2 *Summary of differentially expressed genes between the 5-Aza-dC[a] treated and untreated NB cell line*

Affymetrix probe set ID	Gene symbol	Fold change[b]	Chromosome	Description
Apoptosis				
215719_x_at	TNFRSF6	4.03	10q24.1	Tumor necrosis factor receptor superfamily
202284_s_at	CDKN1A	3.91	6p21.2	Cyclin-dependent kinase inhibitor 1A
211078_s_at	STK3	3.73	8q22.2	Serine/threonine kinase 3
Cell adhesion				
201109_s_at	THBS1	18.68	15q15	Thrombospondin 1
207315_at	CD226	15.26	18q22.3	CD226 antigen
219738_s_at	PCDH9	3.36	13q14.3-q21.1	Protocadherin 9
207717_s_at	PKP2	−5.18	12p11	Plakophilin 2
Transcription regulation				
206830_at	SLC4A10	6.54	2q23-q24	Solute carrier family 4,
203081_at	CTNNBIP1	4.53	1p36.22	Catenin, β interacting protein 1
214009_at	MSL3L1	3.62	Xp22.3	Male-specific lethal 3-like 1 (*Drosophila*)
204349_at	CRSP9	3.44	5q33.3	Cofactor required for Sp1 transcriptional activation
205092_x_at	ZBTB1	3.28	14q23.3	Zinc finger and BTB domain containing 1
206644_at	NR0B1	−3.02	Xp21.3-p21.2	Nuclear receptor subfamily 0, group B, member 1
206543_at	SMARCA2	−3.42	9p22.3	Actin-dependent regulator of chromatin
206035_at	REL	−4.65	2p13-p12	V-rel reticuloendotheliosis viral oncogene homolog
220844_at	TCEB3L	−5.46	18q21.1	Transcription elongation factor (SIII) elongin A2
205688_at	TFAP4	−7.63	16p13	Transcription factor AP-4
Signal transduction				
214586_at	GPR37	6.97	7q31	G protein-coupled receptor 37
206584_at	LY96	4.02	8q13.3	Lymphocyte antigen 96
205280_at	GLRB	3.35	4q31.3	Glycine receptor, β
207859_s_at	CHRNB3	−3.32	8p11.2	Cholinergic receptor, nicotinic, βpolypeptide 3
219898_at	GPR85	−3.56	7q31	G protein-coupled receptor 85
215669_at	HLA-DRB3	−7.84	6p21.3	MHC, class II
209920_at	BMPR2	−14.12	2q33-q34	Bone morphogenetic protein receptor, type II
Heat shock response				
207714_s_at	SERPINH1	82.78	11	Heat shock protein 47
200799_at	HSPA1A	10.94	6p21.3	Heat shock 70kDa protein 1A
Transport				
220791_x_at	SCN11A	4	3p24-p21	Sodium channel, voltage-gated, type XI, α
212907_at	SLC30A1	3.37	1q32-q41	Solute carrier family 30, member 1
207928_s_at	GLRA3	−3.41	4q33-q34	Glycine receptor, α3
214337_at	COPA	−3.47	1q23-q25	Coatomer protein complex, subunit α
Immune response				
206513_at	AIM2	7.43	1q22	Absent in melanoma 2
200904_at	HLA-E	4.11	6p21.3	MHC, class I, E
202490_at	IKBKAP	3.32	9q34	Inhibitor of κ light polypeptide gene enhancer
215669_at	HLA-DRB3	−7.84	6p21.3	MHC, class II
Organogenesis				
210579_s_at	TRIM10	12.8	6p21.3	Tripartite motif-containing 10
210427_x_at	ANXA2	7.31	15q21-q22	Annexin A2
Metabolism				
219532_at	ELOVL4	5.83	6q14	Elongation of very long chain fatty acids -like 4
207813_s_at	FDXR	3.12	17q24-q25	Ferredoxin reductase
207252_at	UBE1	−3	Xp11.23	Ubiquitin-activating enzyme E1
202015_x_at	METAP2	−13.01	12q23.1	Methionyl aminopeptidase 2
Miscellaneous genes				
219454_at	EGFL6	4.12	Xp22	EGF-like-domain, multiple 6
213397_x_at	RNASE4	3.73	14q11.1	Ribonuclease, RNase A family, 4
38691_s_at	SFTPC	−3.19	8p21	Surfactant, pulmonary-associated protein C
215704_at	FLG	−5.85	1q21	Filaggrin

[a] 5-Aza-dC, 5′-aza-2′-deoxycytidine; NB, neuroblastoma; EGF, epidermal growth factor.
[b] Positive (+) fold change indicates genes up-regulated in the 5-Aza-dC treated NB cell line. Negative (−) fold change indicates genes down-regulated in the 5-Aza-dC treated NB cell line.

with a 1:3000 and 1:50 dilution of primary anti-Hsp47 antibody (Stressgen) and collagen IV antibody (Chemicon), respectively, in a humidity chamber overnight at 4°C, and developed with peroxidase-labeled dextran polymer followed by diaminobenzidine (DAKO Envision Plus System; DAKO Corporation, Carpinteria, CA). For double labeling, sections were incubated with anti-Hsp47 and anticollagen IV antibodies and then developed with diaminobenzidine and 3-amino-9-ethylcarbazole (DAKO Envision Plus System) for Hsp47 and type IV collagen, respectively. Sections were counterstained with Gill's hematoxylin. For negative controls, primary antibody was omitted. Hsp47 and collagen IV staining above the background in the tumor cytoplasm or in the extracellular matrix (ECM) was scored as positive. Histological sections from human GNRs ($n = 6$), ganglioneuroblastomas ($n = 2$), and NBs ($n = 5$) were also immunostained with a mouse anti-type I collagen (1:40 dilution; from the Development Studies Hybridoma Bank) using similar techniques.

RESULTS

Expression Analysis by Microarray. Genome-wide gene expression analysis was performed for control and 5-Aza-dC-treated NBL-W-S NB cells in an effort to identify the genes and signal transduction pathways that are modulated by treatment with this demethylating agent. Differential expression (≥3-fold) was detected for 44 genes; 27 were up-regulated, whereas 17 were down-regulated (Table 2). As expected, *TSP-1* was up-regulated (>18-fold) after treatment with 5-Aza-dC. We also found changes in expression of genes that encode proteins that play roles in apoptosis, cell adhesion, transcriptional regulation, and signal transduction. Significant up-regulation of two heat shock response genes was observed, with a >10% increase in the gene coding for heat shock 70 kDa protein 1A, and a >80-fold increase in the level of expression of *Hsp47* after 5-Aza-dC treatment.

Analysis of *Hsp47* Expression in NB Cell Lines. To confirm that disrupting methylation would induce *Hsp47* expression in NB cells, as the microarray results suggested, the expression of this gene was additionally characterized by reverse transcription-PCR in control and 5-Aza-dC-treated NBL-W-S cells. As shown in Fig. 1*A*, *Hsp47* mRNA was not detected in the untreated NB cells, whereas signifi-

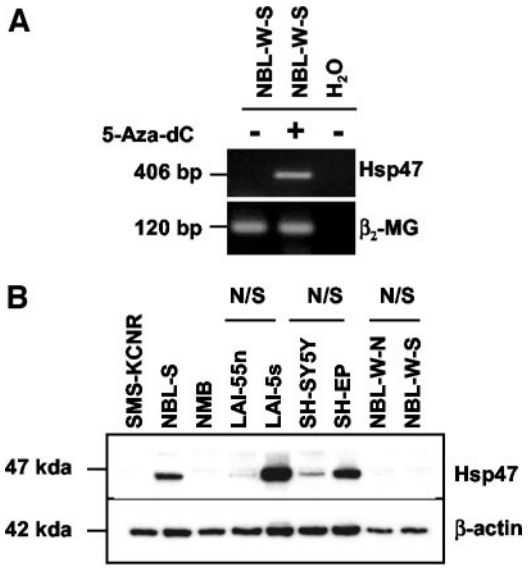

Fig. 1. Expression of *Hsp47* in neuroblastoma (NB) cell lines. *A*, semiquantitative reverse transcription-PCR confirms that *Hsp47* is silenced in NBL-W-S cells. After treatment with 5′-aza-2′-deoxycytidine for 24 h *Hsp47* mRNA expression was restored. *B*, heat shock protein 47 (*Hsp47*) was detected by Western blot analysis in cell lysates from NB cell lines. Higher levels of expression were observed in nontumorigenic Schwannian NB subclones than in tumorigenic NB cell lines and neuronal subclones. Expression of the housekeeping gene *β-actin* was used as a loading control.

cantly increased levels of transcript were seen after treatment with 5-Aza-dC for 24 h. To investigate whether *Hsp47* was silenced in other NB cell lines, we examined Hsp47 protein expression in a panel of 9 NB cell lines by Western blot analyses. We found that in addition to NBL-W-S, 3 other cell lines had undetectable levels of Hsp47 (SMS-KCNR, NMB, and NBL-W-N), whereas 2 cell lines expressed very low levels of Hsp47 (LA1–55n and SH-SY5Y; Fig. 1*B*). Interestingly, high levels of Hsp47 were present in the nontumorigenic S-type NB subclones LA1–5s and SH-EP, whereas all of the cell lines with low to undetectable levels of Hsp47 protein are highly tumorigeneic in nude mice (8, 21, 22).

Methylation and Silencing of the *Hsp47* Promoter in NB Cell Lines and Tumors. Using MSP, we next examined the methylation status of the 5′ flanking region of the *Hsp47* promoter and the region around the transcriptional start site. Fig. 2*A* illustrates the location of the primers used in these assays and the corresponding CpG islands in the *Hsp47* promoter. Genomic DNA was isolated from 3 Hsp47-negative NB cell lines (NMB, NBL-W-S, and NBL-W-N), 2 NB cell lines that express low levels of Hsp47 (LA1–55n and SH-SY5Y), and 3 NB cell lines that express high levels of *Hsp47* (LA1–5s, SH-EP, and NBL-S). The MSP studies demonstrated that the *Hsp47* CpG sites in the transcriptional start site region downstream of the TATA box between bp −24 and +85 were methylated in all 3 of the Hsp47-negative cell lines, whereas these sites were completely unmethylated in the LA1–5s and SH-EP cell lines that express high levels of Hsp47 (Fig. 2*B*). Both methylated and unmethylated alleles were detected in LA1–55n and SH-SY5Y cells, although the intensity of the unmethylated band was much stronger than that of the methylated band. A similar pattern of methylation was observed in these cell lines when the MSP analysis was performed using primers corresponding to the 5′ flanking region between bp −351 and −218 (data not shown). To investigate whether aberrant methylation also occurred *in vivo*, the methylation status of the *Hsp47* promoter was analyzed in NB tumor samples. As shown in Fig. 2*C*, methylation in the region of the

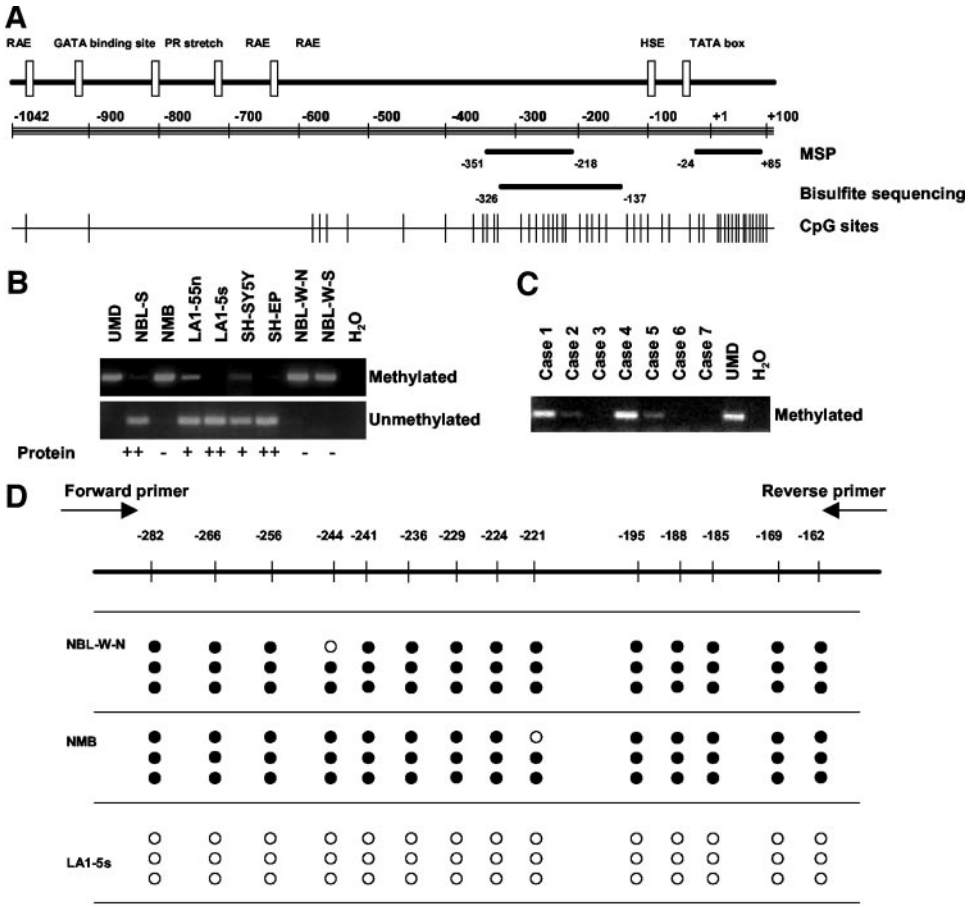

Fig. 2. Methylation status of the *Hsp47* gene in neuroblastoma (NB) cell lines and clinical tumors. *A*, promoter region of *Hsp47* gene and location of PCR primers used in this study. The *numbering* indicates the nucleotide position relative to the transcriptional start site, which is designated +1. *Short vertical bars on the bottom line* show CpG sites. *B*, methylation status of *Hsp47* in the region between −24 to +85 around the transcriptional start site was characterized in *Hsp47*-positive and -negative NB cell lines using methylation-specific PCR (*MSP*). Universal methylated DNA (*UMD*) was used as a positive control. *C*, methylation status of *Hsp47* around transcriptional start site was characterized in NB primary tumors using MSP. *D*, bisulfite sequencing analysis of 5′-flanking region of *Hsp47* gene. Plasmid clones bearing bisulfite-modified fragment of Hsp47 promoter from −326 to −137 encompassing 14 CpG sites (−282, −266, −256, −244, −241, −236, −229, −224, −221, −195, −188, −185, −169, and −162 from transcriptional start site) were characterized by sequencing. Each *row of circles* represents a single sequenced plasmid containing cloned PCR product of bisulfite-treated genomic DNA. ●, methylated cytosine; ○, unmethylated cytosine.

transcriptional start site of the *Hsp47* promoter was detected in a subset of primary NB tumors.

To additionally confirm the aberrant hypermethylation of the *Hsp47* promoter, bisulfite-specific PCR (−326 to −137) was performed, and products were purified, cloned into the pCR2.1-TOPO vector, and sequenced. All but 1 of the cysteines in the 14 CpG sites evaluated were methylated in the *Hsp47*-negative cell lines NMB and NBL-W-N. In contrast, in the Hsp47-positive cell line LA1–5s, all of the cysteines in the CpG islands were unmethylated (Fig. 2*D*). Cysteines at non-CpG sites were converted to thymine, excluding the possibility that successful amplification could be attributable to incomplete bisulfite conversion (data not shown).

Coexpression of Hsp47, Collagen I, and Collagen IV in NB Cells. Hsp47 functions as a molecular chaperone for collagen, and its expression has been shown to be closely correlated with collagen production in a number of cell types. As a first step toward determining whether Hsp47 is capable of regulating collagen expression in NB, we double stained 4 NB cell lines with anti-Hsp47 and anticollagen I or IV antibodies, and used FITC- and rhodamine-conjugated secondary antibodies. In the Hsp47-positive cell lines SH-EP and LA1–5s, collagen type I and type IV were present in the cytoplasm. In contrast, neither collagen was detected in the Hsp47-negative cell lines (NBL-W-N and NMB; Fig. 3, *A* and *B*).

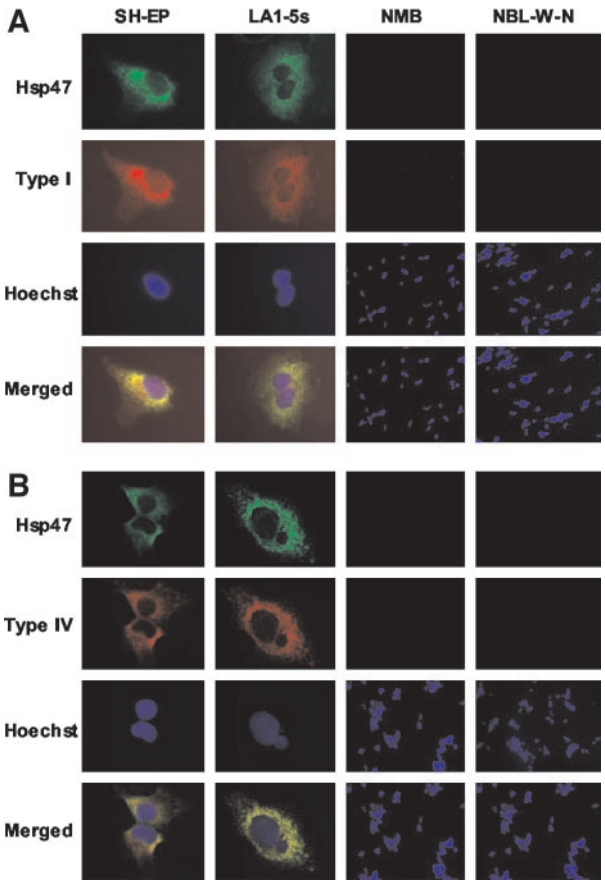

Fig. 3. Expression of heat shock protein (*Hsp*)47 with type I or type IV collagen in neuroblastoma (NB) cell lines was determined by immunofluorescence. *A,* expression of collagen type I in Hsp47-positive and -negative NB cell lines. *B,* expression of collagen IV in Hsp47-positive and -negative NB cell lines. Images were obtained with a LEICA DMIRB microscope separately for Hsp47 and type I or type IV collagen. In the double staining with both FITC and rhodamine images, the *yellow color* indicates the overlap of the two fluorescent antibodies. *Blue color* indicates the Hoechst counterstaining of the nucleus. Positive expression was shown at high magnification (×600); negative staining of multiple cells was shown at low magnification (×150).

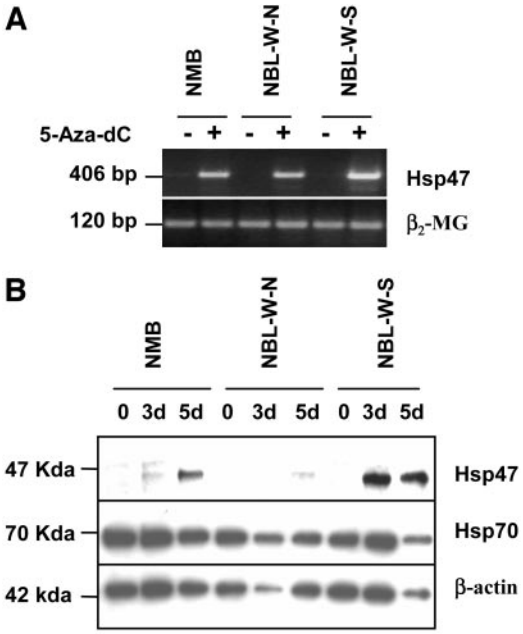

Fig. 4. Restoration of *Hsp47* expression in neuroblastoma (NB) cell lines after treatment with 5′-aza-2′-deoxycytidine (*5-Aza-dC*). *A, Hsp47* gene expression was analyzed by reverse transcription-PCR in untreated NB cell lines and after 4-day treatment with 5-Aza-dC *in vitro*. *B,* Western blot analysis of Hsp47 and Hsp70 expression in cell lysates from NMB, NBL-W-N, and NBL-W-S after treatment with 5-Aza-dC at the indicated times.

Restoration of *Hsp47* Expression in *Hsp47*-Negative Cell Lines by 5-Aza-dC. To investigate whether *Hsp47* expression could be restored in *Hsp47*-negative cell lines (NMB, NBL-W-N, and NBL-W-S), the cell lines were treated with 5-Aza-dC for 4 days. As shown in Fig. 4*A*, Hsp47 mRNA expression was induced in all 3 of the NB cell lines. Moreover, Hsp47 protein was also detected in these cells lines after treatment with 5-Aza-dC for 3 and 5 days, although the level of *Hsp47* expression in the NBL-W-N cell line remained low (Fig. 4*B*). In the NMB and NBL-W-S cells, Hsp47 was up-regulated within 3 days of treatment with the demethylating agent (Fig. 4*B*). No change in the level of Hsp70 protein, another heat shock protein, was seen in these cell lines after treatment with 5-Aza-dC (Fig. 4*B*).

5-Aza-dC Restores *Hsp47* Expression in a Subset of NB Xenografts. Nude mice with xenografts generated from Hsp47-negative NB cell lines (NBL-W-S, NBL-W-N, and NMB) were treated with 5-Aza-dC as described previously (8) to determine whether Hsp47 expression could also be restored *in vivo*. In the treated NBL-W-S xenografts, higher levels of Hsp47 were detected in the cytoplasm of the NB cells compared with the controls (Fig. 5). Moreover, up-regulation of collagen IV was also detected in the ECM of NBL-W-S xenografts. Double labeling studies indicated that Hsp47 and collagen IV were colocalized as visualized by the dark brown color. However no difference in the level of expression of either Hsp47 or collagen IV was detected in NBL-W-N and NMB xenografts after treatment with 5-Aza-dC (data not shown).

Expression of Collagens in NB Cell Lines and NB Primary Tumors. To additionally investigate the relationship between Hsp47 and collagen expression, Western blot analyses were performed with 6 NB cell lines. Both type I and type IV collagen were detected in the NB cell lines that expressed high levels of Hsp47 (LA1–5s and SH-EP). Similar to previous studies, two α1(I) collagen bands corresponding to the propeptide and *N*-propeptide forms of the α1(I) chains were observed (17), and both low- and high-molecular-weight forms of type IV collagen (13) were detected in our experiments. In contrast, collagen was not seen in NB cell lines that express low to undetectable

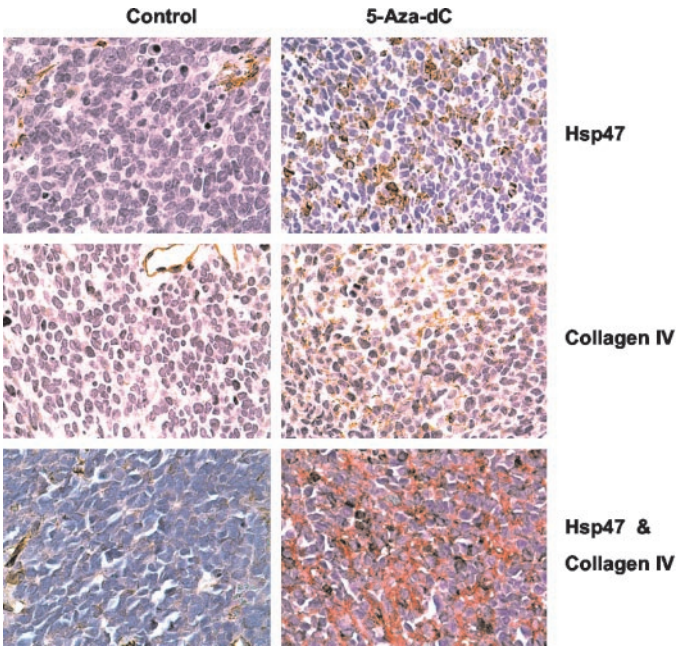

Fig. 5. Up-regulation of heat shock protein (Hsp)47 and collagen IV *in vivo*. Effect of 5′-aza-2′-deoxycytidine (*5-Aza-dC*) on Hsp47 expression in untreated and treated NBL-W-S-derived xenografts was detected by immunohistochemistry staining using anti-Hsp47 antibody (*top, brown color;* magnification ×400). Collagen IV expression was detected in 5-Aza-dC untreated and treated NBL-W-S xenografts with anticollagen IV antibody (*middle, red color;* magnification ×400). Immunohistochemistry using double-labeling showed that up-regulation of collagen IV can be detected in Hsp47-positive xenografts after treatment with 5-Aza-dC (*bottom, dark brown color,* magnification ×400).

levels of Hsp47 (NBL-W-N, NMB, LA1–55n, and SH-SY5Y; Fig. 6*A*). Collagen expression was also examined by Western blot in 7 benign GNRs and 5 clinically aggressive advanced-stage NB tumors. Type I collagen was detected in 6 of the 7 GNRs, whereas low to undetectable levels of collagen expression were present in the 5 advanced-stage tumors (Fig. 6*B*). Immunohistochemistry studies similarly demonstrated higher levels of type I collagen expression in GNRs and ganglioneuroblastomas compared with undifferentiated NBs (Fig. 6*C*). In the histologically mature tumors, both ganglion cells and differentiated neuroblasts expressed type I collagen. In contrast, collagen was not detected in tumors composed of undifferentiated neuroblasts. Type I collagen expression was also detected in the Schwann cells in a GNR by immunofluorescence using antibodies directed against collagen type I and S-100 (Fig. 6*C*). In addition, Western blot analyses revealed type I collagen in CM prepared from Schwann cells, further demonstrating that Schwann cells are capable of secreting this protein (Fig. 6*D*).

DISCUSSION

Multiple genes have been shown to be hypermethylated and silenced in NB (9–12). We demonstrated recently that the antiangiogenic factor gene *TSP-1* is methylated in NB and that treatment with the demethylating agent 5-Aza-dC restored *TSP-1* expression and inhibited significantly NB growth *in vivo* (8). In an effort to identify the genes, in addition to *TSP-1*, that are responsible for the impaired NB tumor growth observed after treatment with 5-Aza-dC, we performed genome-wide gene expression analysis of control and treated NBL-W-S NB cells. Forty-four genes were detected that displayed ≥3-fold differential levels of expression between control and treated NBL-W-S NB cells. *TSP-1* provided an internal control for the microarray studies, and, as expected, this gene was significantly up-regulated in experiments performed with the 5-Aza-dC-treated NB cells. In addition, alterations in the levels of expression of genes that encode cell adhesion molecules and proteins that play a role in transcription regulation, signal transduction, immune response, or apoptosis were observed. The gene encoding Hsp47, a collagen-specific molecular chaperone, displayed the highest level of differential expression, with >80-fold increase in expression after treatment with the demethylating agent. As a first step toward investigating

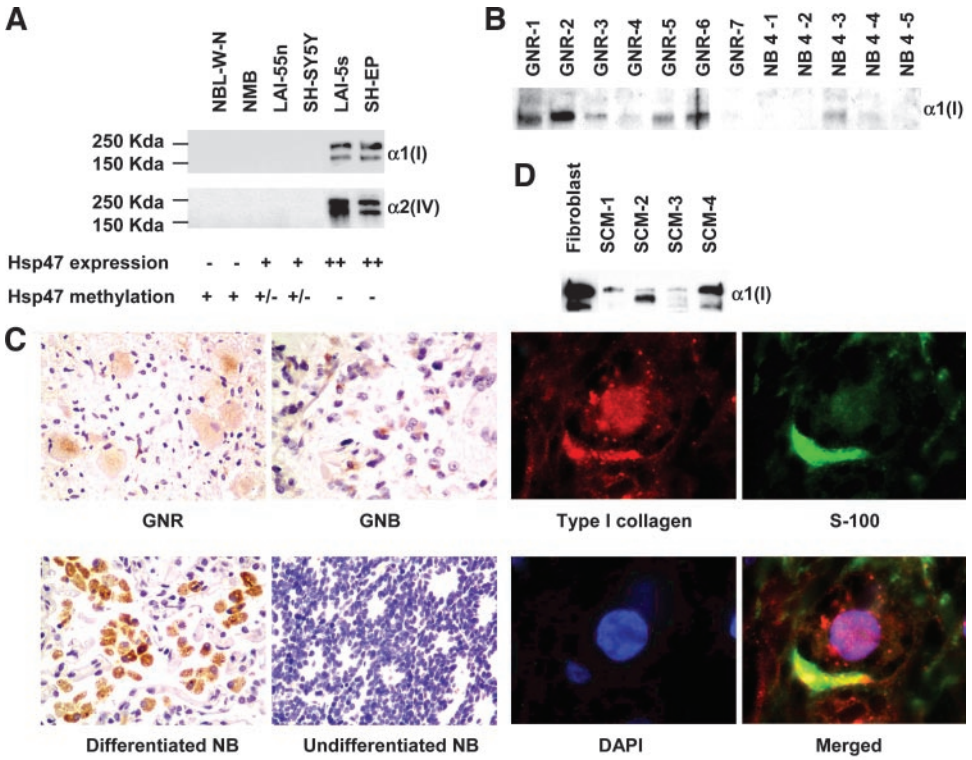

Fig. 6. Expression of collagen in neuroblastoma (NB) cell lines and primary tumors. *A,* expression of type I and IV collagen in NB cell lines was determined by Western blot using mouse monoclonal anti-pro-α1(I) NH_2-terminal propeptide and α2(IV) antibodies. *B,* expression of type I collagen in ganglioneuromas (*GNR*) and advanced-stage NB tumors was determined using a mouse monoclonal anti-pro-α1(I) NH_2-terminal propeptide antibody. *C,* expression of type I collagen in GNRs, ganglioneuroblastomas (*GNB*), and advanced-stage, undifferentiated NB tumors was determined by immunohistochemistry (magnification ×400). Type I collagen expression in Schwann cells was determined by immunofluorescence using double labeling with anti-pro-α1(I) NH_2-terminal propeptide and S-100 antibodies (magnification ×630). Ganglion cells are type I collagen positive and S-100 negative. The *yellow color* indicates the overlap of positivity of the two fluorescent antibodies. *Blue color* indicates the 4′,6-diamidino-2-phenylindole counterstaining of the nucleus. *D,* expression of secreted type I collagen was detected in conditioned media generated from Schwann cells by Western blot analyses.

whether the significant induction of *Hsp47* after treatment with 5-Aza-dC impacted the biological behavior of NB, its pattern of expression in NB and mechanisms of regulation were additionally evaluated.

Expression studies confirmed that *Hsp47* was silenced in NBL-W-S cells as well as in a subset of other NB cell lines. A typical CpG island is present at the 5′ flanking region of *Hsp47* and in the region around the transcriptional start site. MSP and bisulfite sequencing revealed that the promoter region of the *Hsp47* gene was methylated in a subset of NB cell lines and primary tumors, and the methylation status was found to be inversely associated with gene expression. Although another member of the heat shock protein family, *Hsp70*, has been shown to be methylated in primary mouse embryo cells and murine cell lines (23), to our knowledge this is the first report of aberrant methylation of *Hsp47*. We also found that treatment with 5-Aza-dC restored *Hsp47* expression in Hsp47-negative cell lines *in vitro*, and up-regulation of Hsp47 was detected in a subset of NB xenografts after administration of 5-Aza-dC *in vivo*.

In a number of cell types, Hsp47 has been shown to specifically and transiently bind to newly synthesized procollagens, and recent studies indicate that Hsp47 is required to form the rigid triple-helical structure characteristic of mature type I collagen (13–15, 24). Immunofluorescence was used to evaluate collagen expression, and consistent with its role as a collagen molecular chaperone, we found coexpression of Hsp47 with types I and IV collagen in the cytoplasm of NB cells. In contrast, NB cells with low to undetectable levels of Hsp47 did not express collagen. Furthermore, both Hsp47 and collagen IV were up-regulated in NBL-W-S-derived NB xenografts after treatment with 5-Aza-dC, supporting a role for Hsp47 in collagen production in NB.

Although it remains unclear whether Hsp47 and/or type I and type IV collagen directly influence NB growth, high levels of Hsp47 and collagen were detected in nontumorigenic NB subclones. In contrast, this gene was silenced or only detected at low levels in tumorigenic NB cell lines. We also found high levels of secreted types I and IV collagen in the CM collected from the nontumorigenic NB cell lines, whereas collagen was not seen in the CM collected from tumorigenic cell lines. In addition, enhanced levels of Hsp47 and collagen type IV were detected in a subset of the 5-Aza-dC-treated NB xenografts that displayed impaired tumor growth (8). In primary tumors, type I collagen was expressed in mature GNRs and ganglioneuroblastomas, whereas type I collagen was not detected in more clinically aggressive NB tumors composed of undifferentiated neuroblasts, additionally suggesting that collagen may play a role in influencing NB phenotype. Similarly, previous studies have indicated that collagen may negatively impact the malignant potential of other types of cancer. The level of Hsp47 and type I collagen expression is decreased after the malignant transformation of fibroblasts (14, 25). In addition, Hsp47 and type IV collagen are markedly increased during the differentiation of a mouse teratocarcinoma cell line (15). Furthermore, in head and neck carcinomas, lower levels of collagen XVIII and endostatin, an antiangiogenic molecule derived from collagen XVIII after cleavage, are detected in primary head and neck tumors from patients with metastatic disease compared with nonmetastatic cases (26).

The ECM, which is largely composed of type I collagen, is known to negatively regulate normal cell proliferation. Although much less is known about the growth regulatory effects of the ECM on malignant cells, several lines of evidence suggest that collagen and/or collagen fragments are capable of influencing tumor growth. Contact with type I collagen has been shown to growth arrest melanoma cells (27). Similarly, using a three-dimensional ECM that is rich in type I collagen, Hotary *et al.* (28) demonstrated that the proliferation of tumor cells suspended in three-dimensional gels consisting of protease-resistant type I collagen was fully suppressed. Animal studies also indicate that the composition of the ECM can modulate tumor growth. Secreted protein acidic and rich in cysteine (SPARC)-null mice display alterations in the production and organization of collagen in the ECM, and recent studies show that tumors implanted in these mice exhibit enhanced growth and metastases compared with controls (29). The increased tumor growth was believed to be due, at least in part, to the more permissive environment of the SPARC-null mice. In addition to intact collagen, proteolytic fragments of noncollagenous domains of collagens IV, XV, and XVIII may also influence tumor growth by inhibiting angiogenesis (30–34).

In NB, treatment with the demethylating agent 5-Aza-dC leads to alterations in the level of expression of several genes that are likely to be involved in the regulation of tumor growth. Although the roles that Hsp47 and collagen may play in NB pathogenesis are not known, our results and those reported by others suggest that Hsp47 regulates the production of collagen and that collagen and its cleavage fragments may negatively influence the malignant potential of NB and other types of cancer. Additional functional studies are ongoing in our laboratory to investigate whether NB tumor growth can be directly impacted by contact with type I or IV collagen. Hopefully, these experiments will enhance our understanding of the molecular mechanisms underlying collagen synthesis and function in NB and provide insight into how tumor cell behavior can be influenced by the local microenvironment.

REFERENCES

1. Brodeur GM, Maris JM. Neuroblastoma. In: Pizzo PA, Poplack DG, editors. Principles and Practice of Pediatric Oncology, 4 ed. Philadelphia: Lippincott-Raven; 2001. p. 895–937.
2. van Noesel MM, Versteeg R. Pediatric neuroblastomas: genetic and epigenetic 'Danse Macabre'. Gene 2004;325:1–15.
3. Look AT, Hayes FA, Shuster JJ, et al. Clinical relevance of tumor cell ploidy and N-myc gene amplification in childhood neuroblastoma: a Pediatric Oncology Group study. J Clin Oncol 1991;9:581–91.
4. Brodeur GM, Seeger RC, Schwab M, Varmus HE, Bishop JM. Amplification of N-myc in untreated human neuroblastomas correlates with advanced disease stage. Science 1984;224:1121–4.
5. Seeger RC, Brodeur GM, Sather H, et al. Association of multiple copies of the N-myc oncogene with rapid progression of neuroblastomas. N Engl J Med 1985;313:1111–6.
6. Bown N, Cotterill S, Lastowska M, et al. Gain of chromosome arm 17q and adverse outcome in patients with neuroblastoma. N Engl J Med 1999;340:1954–61.
7. Maris JM, Matthay KK. Molecular biology of neuroblastoma. J Clin Oncol 1999;17: 2226–79.
8. Yang QW, Liu S, Tian Y, et al. Methylation-associated Silencing of the Thrombospondin-1 Gene in Human Neuroblastoma. Cancer Res 2003;63:6299–310.
9. Yan P, Muhlethaler A, Bourloud KB, Beck MN, Gross N. Hypermethylation-mediated regulation of CD44 gene expression in human neuroblastoma. Genes Chromosom Cancer 2003;36:129–38.
10. Teitz T, Wei T, Valentine MB, et al. Caspase 8 is deleted or silenced preferentially in childhood neuroblastomas with amplification of MYCN. Nat Med 2000; 6:529–35.
11. van Noesel MM, van Bezouw S, Voute PA, Herman JG, Pieters R, Versteeg R. Clustering of hypermethylated genes in neuroblastoma. Genes Chromosomes. Cancer 2003;38:226–33.
12. Astuti D, Agathanggelou A, Honorio S, et al. RASSF1A promoter region CpG island hypermethylation in phaeochromocytomas and neuroblastoma tumours. Oncogene 2001;20:7573–7.
13. Nagai N, Hosokawa M, Itohara S, et al. Embryonic lethality of molecular chaperone hsp47 knockout mice is associated with defects in collagen biosynthesis. J Cell Biol 2000;150:1499–506.
14. Nagata K, Yamada KM. Phosphorylation and transformation sensitivity of a major collagen-binding protein of fibroblasts. J Biol Chem 1986;261:7531–6.
15. Kurkinen M, Taylor A, Garrels JI, Hogan BL. Cell surface-associated proteins which bind native type IV collagen or gelatin. J Biol Chem 1984;259:5915–22.
16. Jain N, Brickenden A, Ball EH, Sanwal BD. Inhibition of procollagen I degradation by colligin: a collagen-binding serpin. Arch Biochem Biophys 1994;314:23–30.
17. Sauk JJ, Smith T, Norris K, Ferreira L. Hsp47 and the translation-translocation machinery cooperate in the production of alpha 1(I) chains of type I procollagen. J Biol Chem 1994;269:3941–6.
18. Foley J, Cohn SL, Salwen HR, et al. Differential expression of N-myc in phenotypically distinct subclones of a human neuroblastoma cell line. Cancer Res 1991;51: 6338–45.
19. Chlenski A, Liu S, Crawford SE, et al. SPARC is a key Schwannian-derived inhibitor controlling neuroblastoma tumor angiogenesis. Cancer Res 2002;62:7357–63.

20. Cohn SL, London WB, Huang D, et al. MYCN expression is not prognostic of adverse outcome in advanced-stage neuroblastoma with nonamplified MYCN. J Clin Oncol 2000;18:3604–13.
21. Biedler JL, Spengler BA, Chang TD, Ross RA. Transdifferentiation of human neuroblastoma cells results in coordinate loss of neuronal and malignant properties. Prog Clin Biol Res 1988;271:265–76.
22. Ciccarone V, Spengler BA, Meyers MB, Biedler JL, Ross RA. Phenotypic diversification in human neuroblastoma cells: expression of distinct neural crest lineages. Cancer Res 1989;49:219–25.
23. Gorzowski JJ, Eckerley CA, Halgren RG, Mangurten AB, Phillips B. Methylation-associated transcriptional silencing of the major histocompatibility complex-linked hsp70 genes in mouse cell lines. J Biol Chem 1995;270:26940–9.
24. Saga S, Nagata K, Chen WT, Yamada KM. pH-dependent function, purification, and intracellular location of a major collagen-binding glycoprotein. J Cell Biol 1987;105:517–27.
25. Nakai A, Hirayoshi K, Nagata K. Transformation of BALB/3T3 cells by simian virus 40 causes a decreased synthesis of a collagen-binding heat-shock protein (hsp47). J Biol Chem 1990;265:992–9.
26. Nikitakis NG, Rivera H, Lopes MA, et al. Immunohistochemical expression of angiogenesis-related markers in oral squamous cell carcinomas with multiple metastatic lymph nodes. Am J Clin Pathol 2003;119:574–86.
27. Henriet P, Zhong ZD, Brooks PC, Weinberg KI, DeClerck YA. Contact with fibrillar collagen inhibits melanoma cell proliferation by up-regulating p27KIP1. Proc Natl Acad Sci USA 2000;97:10026–31.
28. Hotary KB, Allen ED, Brooks PC, Datta NS, Long MW, Weiss SJ. Membrane type I matrix metalloproteinase usurps tumor growth control imposed by the three-dimensional extracellular matrix. Cell 2003;114:33–45.
29. Brekken RA, Puolakkainen P, Graves DC, Workman G, Lubkin SR, Sage EH. Enhanced growth of tumors in SPARC null mice is associated with changes in the ECM. J Clin Invest 2003;111:487–95.
30. Hamano Y, Zeisberg M, Sugimoto H, et al. Physiological levels of tumstatin, a fragment of collagen IV alpha3 chain, are generated by MMP-9 proteolysis and suppress angiogenesis via alphaV beta3 integrin. Cancer Cell 2003;3:589–601.
31. Maeshima Y, Sudhakar A, Lively JC, et al. Tumstatin, an endothelial cell-specific inhibitor of protein synthesis. Science 2002;295:140–3.
32. Ramchandran R, Dhanabal M, Volk R, et al. Antiangiogenic activity of restin, NC10 domain of human collagen XV: comparison to endostatin. Biochem Biophys Res Commun 1999;255:735–9.
33. Sasaki T, Larsson H, Tisi D, Claesson-Welsh L, Hohenester E, Timpl R. Endostatins derived from collagens XV and XVIII differ in structural and binding properties, tissue distribution and anti-angiogenic activity. J Mol Biol 2000;301:1179–90.
34. O'Reilly MS, Boehm T, Shing Y, et al. Endostatin: an endogenous inhibitor of angiogenesis and tumor growth. Cell 1997;88:277–85.

Methylation-Associated Silencing of the *Heat Shock Protein 47* Gene in Human Neuroblastoma

Qiwei Yang, Shuqing Liu, Yufeng Tian, et al.

Cancer Res 2004;64:4531-4538.